

Direct laser writing of micro-supercapacitors on hydrated graphite oxide films

Wei Gao¹, Neelam Singh², Li Song², Zheng Liu², Arava Leela Mohana Reddy², Lijie Ci², Robert Vajtai², Qing Zhang³, Bingqing Wei³ and Pulickel M. Ajayan^{1,2*}

Microscale supercapacitors provide an important complement to batteries in a variety of applications, including portable electronics. Although they can be manufactured using a number of printing and lithography techniques^{1–3}, continued improvements in cost, scalability and form factor are required to realize their full potential. Here, we demonstrate the scalable fabrication of a new type of all-carbon, monolithic supercapacitor by laser reduction and patterning of graphite oxide films. We pattern both in-plane and conventional electrodes consisting of reduced graphite oxide with micrometre resolution, between which graphite oxide serves as a solid electrolyte^{4–9}. The substantial amounts of trapped water in the graphite oxide makes it simultaneously a good ionic conductor and an electrical insulator, allowing it to serve as both an electrolyte and an electrode separator with ion transport characteristics similar to that observed for Nafion membranes^{10,11}. The resulting micro-supercapacitor devices show good cyclic stability, and energy storage capacities comparable to existing thin-film supercapacitors¹.

Graphite oxide (GO) has recently attracted a great deal of attention, because it offers a low-cost, scalable and wet-chemical approach to graphene^{12–16}. The conductivity of GO, which is dominated by ionic conductivity, depends on the environment and varies between $5 \times 10^{-6} \text{ S cm}^{-1}$ and $4 \times 10^{-3} \text{ S cm}^{-1}$ (refs 8 and 17), suggesting that GO is close to being electrically insulating. Here, we demonstrate that hydrated GO offers very interesting applications in energy storage devices when water is entrapped during processing or is absorbed following exposure to the environment or moisture. When a substantial amount of water is entrapped in the layered GO structure⁹, it becomes a strongly anisotropic ionic conductor as well as an electrical insulator, enabling its use as a viable electrolyte and electrode separator. The ability to laser-reduce GO into conducting reduced graphite oxide (RGO) allows the facile and non-toxic writing of RGO–GO–RGO patterns in various configurations to build electrical double-layer capacitors (EDLC) or supercapacitors.

Recent reports^{18,19} describe the laser reduction conversion of GO into RGO with different levels of reduction and various electrical conductivity improvements. It is possible to pattern any GO surface into RGO–GO–RGO structures in various geometries with micrometre resolution. We constructed both in-plane and conventional sandwich supercapacitor designs, in a number of patterns and shapes as described in Fig. 1 and Supplementary Fig. S1. All the proposed configurations of supercapacitor, conventional sandwich-like configuration and novel in-plane configurations can be directly built on a single piece of GO paper. The as-prepared laser-patterned devices (RGO–GO–RGO) demonstrate good electrochemical performance without the use of an external electrolyte

(Fig. 2). Because of uncertainty in the measurement of the exact mass of the laser-reduced active electrode material, we will mainly report the capacitance values in area and volume density units. The measured capacitance seems to depend on the geometry of the design, as the ionic mobilities and transport distances (thickness of the separator section) are anisotropic and differ for different geometries. The in-plane supercapacitor structure with a circular geometry gives the highest capacitance (0.51 mF cm^{-2}), nearly twice that of the sandwich structure (Fig. 2a). A control experiment was carried out with pristine hydrated GO films and current collectors (with no reduced RGO part), and no capacitance was detectable. The equivalent series resistance (ESR) values obtained from the impedance spectra offer information about how fast the cells are charged/discharged. The in-plane structure has a higher ESR value than the sandwich structure ($6.5 \text{ k}\Omega$ versus 126Ω ; Fig. 2b), indicating it has a lower charge/discharge rate (Supplementary Fig. S2a,b). A recently reported well-designed, inkjet-printed carbon supercapacitor with interdigitated electrode structure and similar electrode thickness had a mean capacitance density of 0.4 mF cm^{-2} with an organic electrolyte¹⁸, showing that the performance of our device, without an external electrolyte, is in the same range as reported for other systems. For electrochemical double-layer microcapacitors, typical capacitance values reported in the literature fall between ~ 0.4 and 2 mF cm^{-2} (ref. 3).

The ionic conductivity of hydrated GO was calculated from the impedance spectra obtained for the devices (see Methods for details)²⁰, giving values of $1.1 \times 10^{-5} \text{ S cm}^{-1}$ for the sandwich geometry and $2.8 \times 10^{-3} \text{ S cm}^{-1}$ for the in-plane one. This anisotropy can be easily explained by the microscopic GO sheet arrangement shown in Supplementary Fig. S2. The hydrated GO film has an anisotropic structure with a *z*-lattice distance of 0.86 nm (obtained by means of X-ray diffraction (XRD) characterization; Supplementary Fig. S3), so ions can move more easily along the intralayer direction rather than normal to the layers. This is similar to the anisotropic electrical conductivity reported for graphite and GO platelets²¹.

In EDLCs, electrical energy storage is achieved by nanoscopic charge (ion) separation at the interface between the electrode and electrolyte. In our system, the only source of ions is the hydrated GO. The morphology and structure of a GO film is shown in Supplementary Figs S4b and S2c. The higher value of the interlayer spacing (0.86 nm , Supplementary Fig. S3) in hydrated GO than in completely dehydrated GO (reported to be 0.567 nm in ref. 9) is an indication of the high water content within our films. We have characterized the water content in hydrated GO to be $\sim 16 \text{ wt}\%$ by means of Karl–Fischer titration⁸. The interaction between the trapped water and GO layers is key to the ionic conductivity observed here. At low concentration, H_2O molecules bind to GO sheets through a strong intermolecular interaction (hydrogen

¹Department of Chemistry, Rice University, Houston, Texas 77005, USA, ²Mechanical Engineering and Materials Science Department, Rice University, Houston, Texas 77005, USA, ³Department of Mechanical Engineering, University of Delaware, Newark, Delaware 19716, USA. *e-mail: ajayan@rice.edu

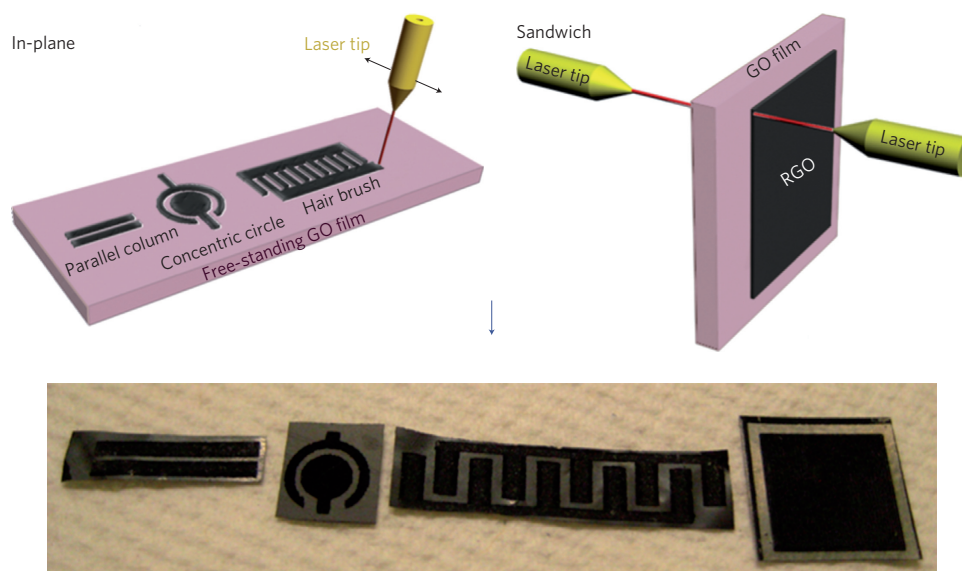


Figure 1 | Schematics of CO₂ laser-patterning of free-standing hydrated GO films to fabricate RGO-GO-RGO devices with in-plane and sandwich geometries. The black contrast in the top schematics corresponds to RGO, and the light contrast to unmodified hydrated GO. For in-plane devices, three different geometries were used, and the concentric circular pattern gives the highest capacitance density. The bottom row shows photographs of patterned films. Typical dimensions of these devices are mentioned in the caption to Supplementary Fig. S1.

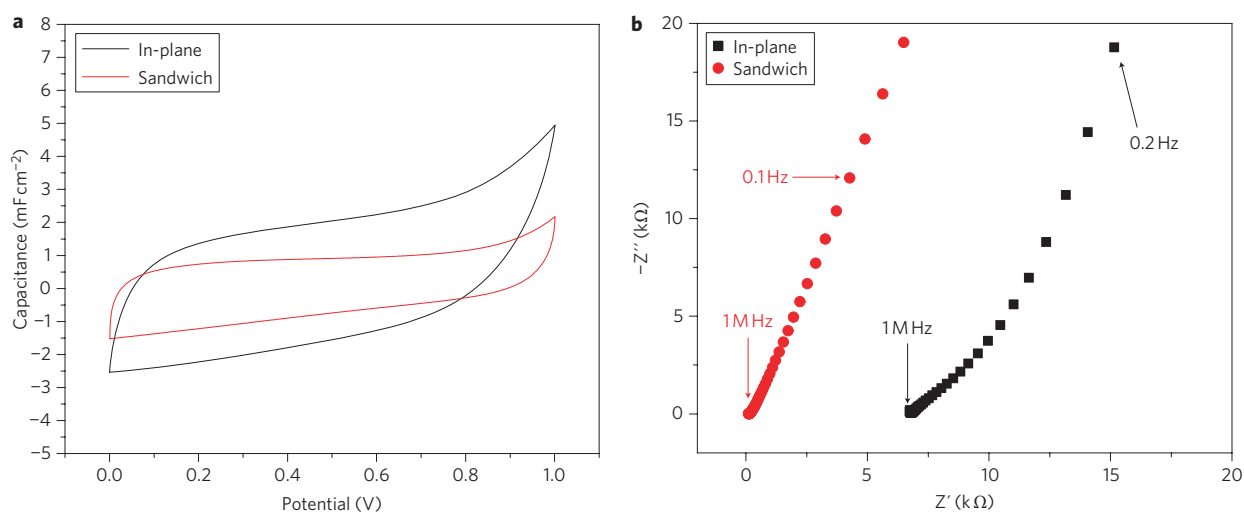


Figure 2 | Comparisons of CV and impedance behaviour of in-plane and sandwich devices. **a**, CV curves of in-plane circular and sandwich devices at a scan rate of 40 mV s^{-1} . The in-plane circular structure gives a specific capacitance twice that of the sandwich structure. **b**, Impedance spectra from 1 MHz to 10 mHz at 10 mV sinusoidal signal, zoomed in at the high-frequency region, demonstrating a much higher ESR value (the intercept of the slanted straight line with the Z' axis) for the in-plane device than for the sandwich device, leading to a lower power density for the in-plane device. Z' , real part of impedance; Z'' , imaginary part of impedance.

bonding). As the water content increases, the active sites on the GO sheets become saturated, and excess water molecules are free to rotate and diffuse. The water content at the reported transition point between the bonded-water and free-water states is $\sim 15 \text{ wt\%}$ (ref. 9). We speculate that protons, which are the species taking part in ionic conduction, arise from hydrolysis of the functional groups (carboxyl, sulphonic²² and/or hydroxyl) present on GO. The resulting protons are able to move by means of the Grotthuss mechanism²³ (hopping via the hydrogen-bonding network), or even migrate freely in the hydronium form (H_3O^+) within the intra-layer spaces (Supplementary Fig.S2). This proton transport seems to be similar to that observed in Nafion, a well-investigated polymer system that demonstrates water-induced proton transport following a hopping mechanism²⁴.

To study the dehydration–rehydration influence on pristine hydrated GO films, impedance spectroscopy measurements were conducted on the films (see Methods) while controlling the environment (under vacuum and at various humidity levels). A stepwise decrease in ionic conductivity (Fig. 3a) is observed with increasing exposure time to vacuum, and a full recovery is seen after re-exposure to air for 3 h. The ionic conductivity calculated from the impedance spectra versus exposure time plot is shown in Fig. 3b. After 6 h under vacuum, there is a two orders of magnitude decrease in the ionic conductivity of the device, which is also fully recovered after exposure to air, indicating the reversibility of this process at room temperature. To study the effect of moisture on the ionic conductivity of GO, impedance spectra measurements were conducted for the GO film at various humidity levels

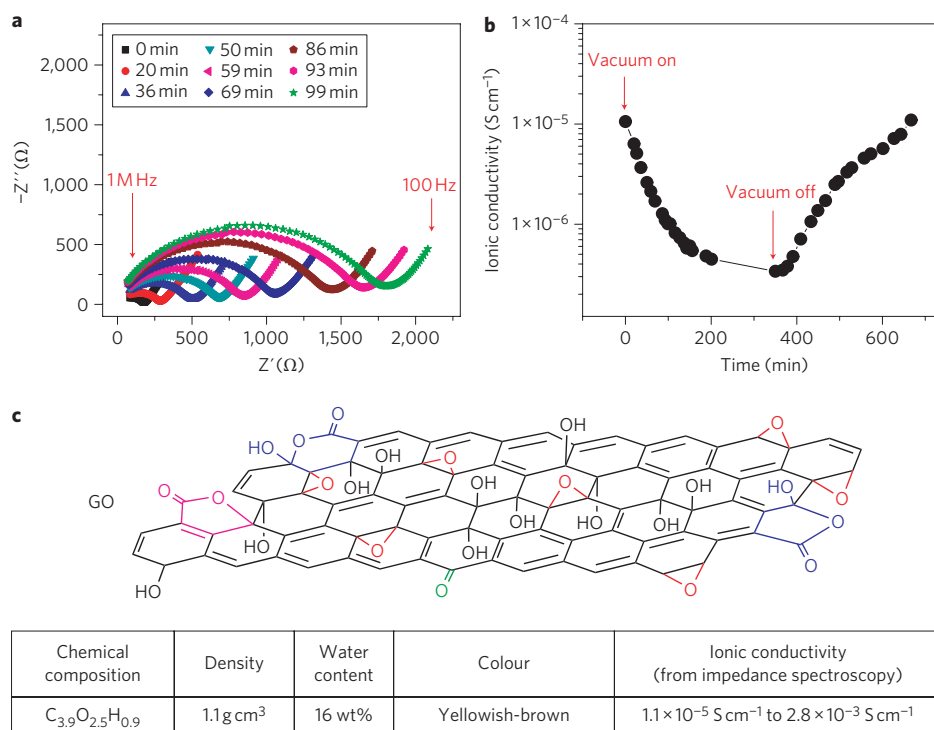


Figure 3 | Characterization of the water effect on GO ionic conductivity. **a**, Stepwise change in impedance spectra versus exposure time to vacuum (0.08 MPa) at 25 °C. Cell structure: a pristine GO film coated with silver on both sides, and sandwiched between two pieces of stainless steel foil (1 cm × 1.2 cm); frequency range, 1 MHz to 100 Hz at 10 mV sinusoidal signal. Water is slowly evaporated out of the film under vacuum, leading to an increase in the arc diameter in the high-frequency range, which indicates a decrease in ionic conductivity. **b**, Dependence of ionic conductivity on exposure time to vacuum and air. Conductivity data were obtained from Z view fitting of the impedance spectra. The hydrated GO film became less conductive under vacuum, but recovered its full conductivity after 3 h of re-exposure to air. Four-probe electrical measurement on a single piece of pristine GO film also showed at least three orders of magnitude decrease in conductance under vacuum (Supplementary methods), indicating that in GO the major contribution to measured conductivity is ionic. **c**, Schematic of GO chemical structure, and table of measured physical properties of GO in an ambient environment. A sandwich geometry with well-defined cross-sectional area offered an accurate conductivity value of $1.1 \times 10^{-5} \text{ S cm}^{-1}$, and the in-plane structure with an estimated cross-sectional area showed a higher ionic conductivity of $2.8 \times 10^{-3} \text{ S cm}^{-1}$. We believe, due to the lamella structure of GO, its ionic conductivity is anisotropic. Upon hydration, the ionic conductivity further increases (Supplementary Fig. S4a,b), and becomes comparable to Nafion¹⁰.

(Supplementary Fig. S4a,b). Almost three orders of change in magnitude of ionic conductivity was observed following hydration of the GO film (Supplementary Fig. S4b). The dramatic changes in ionic conductivity resemble the proton-conducting behavior of Nafion²⁴. The chemical structure and properties of GO and Nafion are shown in Fig. 3c and Supplementary Fig. S4, respectively. The active group in Nafion is a sulphonic acid group²⁵, but in GO it could be a carboxylic acid group, a sulphonic acid group²² or even a tertiary alcohol group. Furthermore, the large number of existing epoxy groups in GO could help proton migration. The application of Nafion as an electrolyte and separator in supercapacitor devices has been reported¹¹. Our observations in relation to the Nafion-like conduction of hydrated GO strongly suggest that it is acting like an ionic conductor, with its ionic/proton conductivity influenced by the water content.

The fact that GO can be easily converted to RGO by means of laser radiation enables any number of in-plane or sandwiched RGO-GO-RGO supercapacitor devices to be produced in a scalable and simple manner via laser-patterning of hydrated GO. The active electrode material RGO, formed from hydrated GO using laser heating, is porous due to the gases produced from the decomposition of the functional groups⁸ and water under localized laser heating (Fig. 4b, Supplementary Fig. S1). The dependence of RGO resistivity and reduction depth on laser power is shown in Supplementary Fig. S5, with a decrease in resistivity by up to four orders of magnitude achieved by this laser treatment, which is consistent with previously reported work¹⁸. The long-range ordered

structure²⁶ in RGO (Fig. 4b) facilitates ion diffusion within the electrode. However, the short-range random arrangement of RGO flakes could lead to resistance to ion migration²⁷, as indicated in the impedance spectra (Fig. 2b). The cyclic stability tests performed on the supercapacitor devices are shown in Fig. 4c. After 10,000 cycles, there is an ~30% drop in the capacitance of the in-plane circular device, whereas an ~35% drop is observed for the sandwich devices. The drop in capacitance seen upon cycling is typical of many supercapacitor devices reported in literature^{28,29}. This decline could be due to water loss in the device. Interestingly, the capacitance doubled when the same device, after long cycling, was kept in ambient conditions for a week (Supplementary Fig. S6).

The in-plane circular design shows the highest specific capacitance of $\sim 0.51 \text{ mF cm}^{-2}$. Considering only the active thickness of the electrodes, the volumetric capacitance is $\sim 3.1 \text{ F cm}^{-3}$, with the electrode volume estimated from the thickness of the reduced region (Supplementary Fig. S7). The energy density for this device is calculated to be $\sim 4.3 \times 10^{-4} \text{ W h cm}^{-3}$, with a power density of 1.7 W cm^{-3} . Owing to its lower ESR value, the sandwich device geometry gives a higher power density of $\sim 9.4 \text{ W cm}^{-3}$, although the energy density for this device is lower ($1.9 \times 10^{-4} \text{ W h cm}^{-3}$). A good match between the 20 mV s^{-1} and 40 mV s^{-1} cyclic voltammetry (CV) scan rates (Supplementary Fig. S8) suggests similar ion diffusion paths within this range of scan rates³⁰. However, we did observe a decrease in capacitance when the scan rate was increased to 100 mV s^{-1} . This could be due to the inhomogeneous pore structure within the electrodes or the pseudo-capacitance caused by

